Photonic band gaps analysis of Thue-Morse multilayers made of porous silicon

Luigi Moretti[1], Ilaria Rea[2], Lucia Rotiroti[2], Ivo Rendina[2], Giancarlo Abbate[3], Antigone Marino[3], Luca De Stefano[2]

[1] *DIMET - University "Mediterranea" of Reggio Calabria, Località Feo di Vito, 89060 Reggio Calabria, Italy*

[2] *Institute for Microelectronics and Microsystems – National Council of Research, Department of Naples, Via P. Castellino 111, 80131 Naples, Italy*

[3] *Department of Physical Sciences and INFM-Coherentia, University of Naples Federico II, Via Cinthia M. S. Angelo, 80126 Naples, Italy*

luigi.moretti@na.imm.cnr.it

Abstract: Dielectric aperiodic Thue-Morse structures up to 128 layers have been fabricated by using porous silicon technology. The photonic band gap properties of Thue-Morse multilayers have been theoretically investigated by means of the transfer matrix method and the integrated density of states. The theoretical approach has been compared and discussed with the reflectivity measurements at variable angles for both the transverse electric and transverse magnetic polarizations of light. The photonic band gap regions, wide 70 nm and 90 nm, included between 0 and 30°, have been observed for the sixth and seventh orders, respectively.

OCIS code: (230.4170) Multilayer, (160.4760) Optical properties, (130.0250) Optoelectronics

References and links

1. E. Yablonovitch, "Inhibited spontaneous emission in Solid-State Physics and Electronics," Phys. Rev. Lett. **58**, 2059 (1987).
2. S. John, "Strong localization of photons in certain disordered dielectric superlattices," Phys. Rev. Lett. **58**, 2486 (1987).
3. S. M. Weiss, M. Haurylau, P. M. Fauchet, "Tunable photonic bandgap structures for optical interconnects," Opt. Mater. **27**, 740 (2005).
4. C. M. Soukoulis and E. N. Economou, "Localization in one-dimensional lattices in the presence of incommensurate potentials," Phys. Rev. Lett. **48**, 1043 (1982).
5. A. Bruyant, G. Lérondel, P. J. Reece, and M. Gal, "All-silicon omnidirectional mirrors based on one-dimensional photonic crystal," Appl. Phys. Lett. **82**, 3227 (2003).
6. V. Agarwal and J. A. del Rio, "Tailoring the photonic band gap of a porous silicon dielectric mirror," Appl. Phys. Lett. **82**, 1512 (2003).
7. N. Liu, "Propagation of light waves in Thue-Morse dielectric multilayers," Phys. Rev. B **55**, 3543 (1997).
8. J. M. Luck, "Cantor spectra and scaling of gap widths in deterministic aperiodic systems," Phys. Rev. B **39**, 5834 (1989).
9. M. Dulea, M. Severin and R. Riklund, "Transmission of light through deterministic aperiodic non-Fibonaccian multilayers," Phys. Rev. B **42,** 3680 (1990).
10. L. Dal Negro, M. Stolfi, Y. Yi, J. Michel, X. Duan, L. C. Kimerling, J. LeBlanc and J. Haavisto, "Photon band gap properties and omnidirectional reflectance in Si/SiO_2 Thue–Morse quasicrystals," Appl. Phys. Lett. **84**, 5186 (2004).
11. F. Qui, R. W. Peng, X. Q. Huang, X. F. Hu, Mu Wang, A. Hu, S. S. Jiang and D. Feng, "Omnidirectional reflection of electromagnetic waves on Thue-Morse dielectric multilayers," Europhys. Lett. **68**, 658-663 (2004).
12. L. Canham, *Properties of Porous Silicon*, (London IEE-INSPEC, 1997).
13. L. Dal Negro, C. J. Oton, Z. Gaburro, L. Pavesi, P. Johnson, A. Lagendijk, M. Righini, L. Colocci, and D. Wiersma, "Light transport through the band-edge states of Fibonacci Quasicrystals," Phys. Rev. Lett. **90**, 55501 (2003).
14. V. Agarwal, J. A. Soto-Urueta, D. Becera, M. E. Mora-Ramos, "Light propagation in polytype Thue-Morse structures made of porous silicon," Photonics Nanostruct. Fundam. **3**, 155 (2005).

#69949 - $15.00 USD Received 14 April 2006; revised 13 June 2006; accepted 14 June 2006

15. M. Born, E. Wolf, *Principles of Optics*, (Cambridge University Press, New York, 2001).
16. J. M. Bendickson, J. P. Dowling, M. Scalora, "Analytic expressions for the electromagnetic mode density in finite, one-dimensional, photonic band-gap structures," Phys. Rev. E **53**, 4107 (1996).
17. X. Jiang, Y. Zhang, S. Feng, K. C. Huang, Y. Yi, and J. D. Joannopoulos, "Photonic band gaps and localization in the Thue–Morse structures," Appl. Phys. Lett. **86**, 201110 (2005).

1. Introduction

Dielectric photonic crystal (PhC) structures [1, 2] have recently attracted great attention for their property to forbid the propagation of the light at fixed wavelengths and the intriguing possibility to realize an all-optical integrated circuit which is the basic element of the optical computer [3]. The simplest, one dimensional PhC structure is the Bragg mirror which is made of alternating layers of low (n_A) and high (n_B) refractive index, whose thicknesses satisfy the Bragg condition: $n_A\, d_A+n_B\, d_B=\lambda_0/2$. The Fourier spectrum (FS) of an infinite PhC shows a δ-function peak at those wavevectors corresponding to the reciprocal lattice vectors. On the other hand, an infinite random structure has a nearly homogeneous FS [4]. A quasi-crystal (QC) does not have a geometrical periodicity but is still deterministically generated: this is the reason why it possesses a FS which is intermediate between a periodic and a random structure. Even if these structures do not have a translational symmetry, they show several interesting physical properties such as the band gaps, some resonance frequencies, and some high localized states [4]. From the experimental point of view, one-dimensional QC are more feasible to be fabricated respect to the PhC which strictly require high geometric precision, so that they have recently attracted great attention as possible competitors in photonics [5, 6]. Thue-Morse (T-M) [7] and Fibonacci [8] systems are the most common examples of one dimensional QC. Dielectric T-M multilayers, showing multiple omnidirectional photonic bandgaps (PBGs) in the visible and near infrared range of wavelengths have been already demonstrated using Si/SiO_2 and TiO_2/SiO_2 as high/low refractive index materials [9-11].

In this paper, we have investigated from the theoretical and experimental point of view the T-M S_1-S_7 sequences by exploiting the porous silicon (PSi) technology. Due to the high quality optical response exhibited by the multilayered structures, the PSi is a very attractive material which can be fabricated by a fast and quite simple process. The PSi is, in fact, obtained by the electrochemical etching of the crystalline silicon in a hydrofluoridric acid (HF) based solution. The porosity and the thickness of a single layer are linear functions of the current density and the anodization time for a fixed doping level of the silicon wafer and HF concentration. The refractive index of the PSi film depends on its porosity, and can be calculated in the frame of several effective medium approximations, like the Bruggemann or Maxwell-Garnett models [12]. Fibonacci QC of up to 233 porous silicon layers has been fabricated in order to study the light propagation in aperiodic structures [13]. Agarwal *et al.* have recently exploited the oxidation effect in T-M multilayers up to more than one thousand layers [14].

The transfer matrix method [15] has been used to investigate the reflectivity spectrum for different T-M orders and the electromagnetic density of modes of the T-M sequences and compared with the experimental results.

2. Theory

The T-M one dimensional structure is constituted by the sequence of two layers A and B with refractive index n_A (n_B) and thickness d_A (d_B). Applying the substitution rules A→AB and B→BA [7] we can deduce all subsequent orders, as follow: S_0=A, S_1=AB, S_2=ABBA, S_3=ABBABAAB, S_4=ABBABAABBAABABBA, and so on. The layers number of S_N is 2^N, where N is the T-M order. A non-recursive expression of the T-M sequence is given by assigning the numerical values 1 and 0 to the A and B symbols, respectively:

#69949 - $15.00 USD Received 14 April 2006; revised 13 June 2006; accepted 14 June 2006

$$\begin{cases} S_N(2j) = S_N(j) \\ S_N(2j+1) = 1 - S_N(j) \end{cases} \quad \text{with} \quad j = 0,1 \tag{1}$$

From the Eq. (1), we can perform a discrete Fourier analysis on the T-M S_5, S_7 and S_{12} strings with 32, 128 and 4096 terms, respectively. The Fourier power spectrums (FPS) are plotted in Fig. 1 as function of the percentage sampling frequency q. The FPS of an aperiodic structure is composed by a finite sequence of peaks which changes, differently from that of a periodic structure, as the system length $d_N=2^N$, increases. In particular, the intensity and the distribution of the peaks changes, concentrating the peaks around the two central resonances which correspond to the band gaps. From Fig. 1(c) is well evident that the self-similarity of the T-M geometry also emerges in the fractal behavior of its FPS.

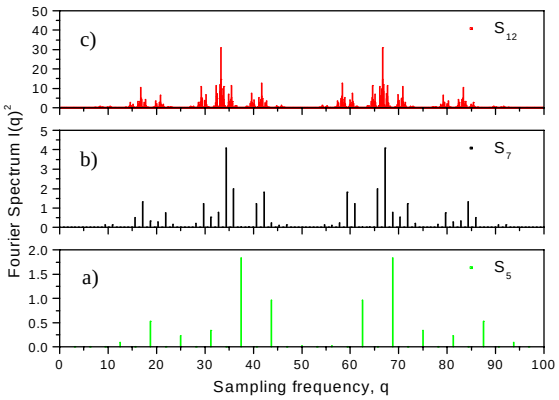

Fig. 1. Fourier power spectrum of the associated T-M strings with 32 (a) 128 (b) and 4096 (c) characters, respectively.

In order to investigate the light propagation properties in a T-M multilayer we define the matrix relation as [15]:

$$\boldsymbol{\chi}(0) = \mathbf{M}(z) \cdot \boldsymbol{\chi}(z) \tag{2}$$

where $\boldsymbol{\chi}(z)$ represents the two-component wave function:

$$\boldsymbol{\chi}(z) = \begin{pmatrix} U(z) \\ V(z) \end{pmatrix} \qquad \text{with} \qquad \begin{cases} \begin{cases} U(z) = E_x \\ V(z) = H_y \end{cases} \text{for TE mode} \\ \begin{cases} U(z) = H_x \\ V(z) = E_y \end{cases} \text{for TM mode} \end{cases} \tag{3}$$

TE and TM represent the transverse-electric and the transverse-magnetic modes, respectively. On the other side $\mathbf{M}(z)$ is described by following relation:

#69949 - $15.00 USD Received 14 April 2006; revised 13 June 2006; accepted 14 June 2006

$$\mathbf{M}_{TE}(z) = \begin{pmatrix} \cos(\phi(z)) & -\dfrac{i}{n\cos(\theta)}\sin(\phi(z)) \\ -i\,n\cos(\theta)\sin(\phi(z)) & \cos(\phi(z)) \end{pmatrix}$$

$$\mathbf{M}_{TM}(z) = \begin{pmatrix} \cos(\phi(z)) & -i\,n\cos(\theta)\sin(\phi(z)) \\ -\dfrac{i}{n\cos(\theta)}\sin(\phi(z)) & \cos(\phi(z)) \end{pmatrix} \tag{4}$$

with $\phi(z) = k_0\, n(z)\, z\cos(\theta)$

$\phi(z)$ is the phase modulation, θ is the incident angle, k_0 is the wave vector in the vacuum, $n(z)$ is the refractive index profile. If an N-th order T-M sequence starts at z_0 and ends at z_N, where z is the stratification direction, we can write:

$$\chi(z_0) = \Gamma_N \cdot \chi(z_N) \tag{5}$$

where Γ_N is the transfer matrix that can be deduced from the following recursion relation:

$$\Gamma_N = \Gamma_{N-1} \cdot \tilde{\Gamma}_{N-1} \quad \text{with} \qquad \Gamma_1 = M_A(d_A) \cdot M_B(d_B) \tag{6}$$

$\tilde{\Gamma}_N$ is the complement of Γ_N obtained by interchanging A and B in Γ_N.

The transmission coefficient, in case of normal incidence, is independent from the polarization light and is given by:

$$t_N = \frac{2}{(\Gamma_{N,11} + \Gamma_{N,12}) + (\Gamma_{N,21} + \Gamma_{N,22})} = x_N + iy_N \tag{7}$$

Bendickson *et al.* [16] demonstrated that for a generic multilayer, the electromagnetic density of mode, $\rho = dk/d\omega$, can be written as function of real and imaginary part of t_N:

$$\rho_N(\omega) = \frac{1}{d_N}\frac{y'_N x_N - x'_N y_N}{x_N^2 + y_N^2} \tag{8}$$

where the prime denotes differentiation with respect to ω. To investigate the photonic band gap properties is advantageous to introduce the integrated density of states (IDOS) defined as:

$$IDOS(\omega) = \frac{\int_0^{\omega} \rho_N(\omega')\, d\omega'}{\int_0^{2\omega_0} \rho_N(\omega')\, d\omega'} \tag{9}$$

This represents the fraction of states whose frequency is smaller than ω, and can be readily determined by numerical calculations. Being the modulation phase $(\phi_A + \phi_B)/\pi = \omega/\omega_0$, the value $2\omega_0$ represent a phase shift of 2π.

#69949 - $15.00 USD Received 14 April 2006; revised 13 June 2006; accepted 14 June 2006

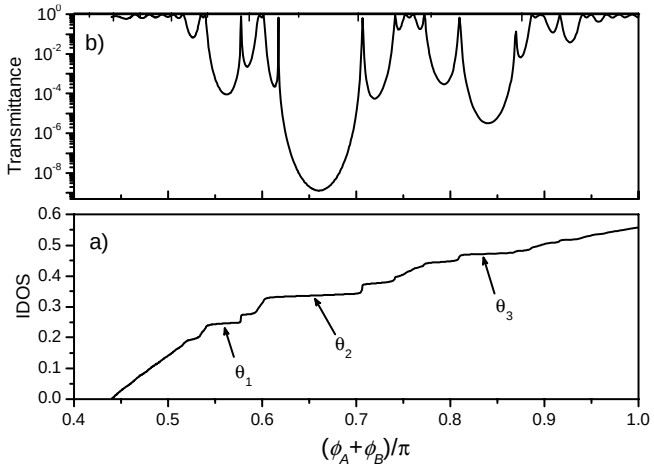

Fig. 2. Plots of Integrated Density Of States (a) and transmittance (b) against the phase (bottom axis) and wavelength (top axis) for S_7 with resonant wavelength λ_0=700 nm. The indicated values of phase correspond to the band gaps discussed in the text.

In Fig. 2 is reported the IDOS of S_7, with a resonance wavelength λ_0 of 700 nm, as function of the wavelength, and its transmittance, $T_N=|t_N|^2$. From the plot of transmittance is interesting to note the same hierarchy peaks of the S_7 FPS in Fig. 1(b). The plateau zones of IDOS represent the band gaps of the T-M structure. The larger band gap is obtained for $(\phi_A+\phi_B)=0.66\pi$ ($\approx 2/3\pi$, θ_2) corresponding with stronger frequency of FPS in Fig. 1(b). Jiang *et al.* identified this gap as a fractal one, which origin is due to the complex correlation depending on the system length [17]. The two small PBGs can be identify approximately at $(\phi_A+\phi_B)=0.57\pi$ (θ_1) and 0.83π (θ_3). Furthermore the strong slopes in IDOS near the PBGs are connected with the narrow transmittance peaks in the S_7 structure, as we can note from the Fig. 2(b).

3. Experiment

A highly doped p^+-silicon, <100> oriented, 0.01 Ω cm resistivity, 400 μm thick was used as the substrate in the T-M structures fabrication. The samples were fabricated in dark light at room temperature using a solution of 30% volumetric fraction of aqueous HF (50% wt) and 70% of Ethanol. Before anodisation, we have removed the thin film of native oxide from the silicon wafer by rapid rinsing in a diluted HF solution. Thicknesses and porosities have been estimated by variable angle spectroscopic ellipsometry (VASE) (J. A. Wollam Company) measurements on single PSi layers.

High porosity layers (p_A=81 %), with an average refractive index $n_A\cong 1.3$ and a thickness $d_A\cong 135$ nm, were obtained applying an etching current density of 150 mA/cm^2 for 0.88 s. Low porosity layers (p_B=56 %), with $n_B\cong 1.96$ and a thickness of $d_B\cong 90$ nm, were obtained with a current density of 5 mA/cm^2 for 0.53 s. The thickness d_i of each layer was designed to satisfy the Bragg condition $n_i d_i=\lambda_0/4$ where n_i is the average refractive index and λ_0=700 nm. A schematic of the PSi T-M sequences realized is reported in Fig. 3: while the number of the layers increases, like 2^N where N is the Thue-Morse order, the thickness of the devices is given by the simple relationship $d_N=2\ d_{N-1}$ for $N>1$. The realized samples S_0-S_7 have thicknesses spanning the range between 0.135 μm and 14.4 μm.

#69949 - $15.00 USD Received 14 April 2006; revised 13 June 2006; accepted 14 June 2006

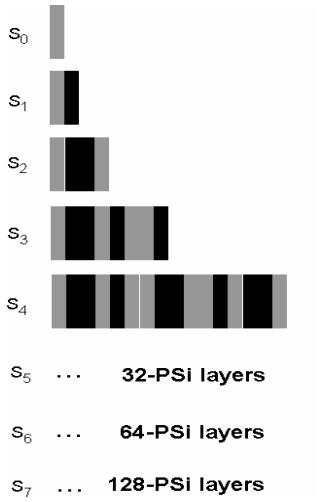

Fig. 3. Schematic of the PSi T-M sequences realized.

A Y optical reflection probe (Avantes), connected to a white light source and to an optical spectrum analyzer (Ando, AQ6315A), has been used for the reflectivity measurements at normal incidence. Samples reflectivity has been characterized as a function of the incident angle by means of the variable angle ellipsometer in the range between 15° and 45° respect to the normal. The input light has been polarized to separate the transverse electric and magnetic components. The reflectivity spectra were measured between 600 and 1600 nm with a resolution of 0.2 nm.

4. Results and discussion

In Figs. 4-5 the experimental (solid curve) and calculated (dashed curve) from Eq. (7) reflectivity spectra for normal incident are shown in case of S_3 [Fig. 4(a)], S_4 [Fig. 4(b)], S_5 [Fig. 4(c)], S_6 [Fig. 5(a)], and S_7 [Fig. 5(b)] T-M structures. The good control in the fabrication process of the devices is demonstrated by the agreement between the measured and calculated spectra. The not perfect matching can be ascribed to the non-uniformities of thicknesses and porosities of layers along the etching direction. The spectrum of the S_3 is characterized by two band gaps separated by a large transmission peak at 1000 nm. On increasing the order of T-M sequence, the PBG splits and very narrow transmission peaks appear (FWHM about 6 nm). The band gap structure, predicted by the numerical calculations, is clearly recognizable at higher the T-M orders. In particular, from the reflectivity spectrum of S_6 in Fig. 5(a) we can distinguish quite clearly the three gaps θ_3, θ_2, and θ_1 that are centered at the wavelengths of 830, 1050 and 1250 nm, respectively. These values of PBGs are in good agreement with the theoretical ones of Fig. 2. On the other hand the S_7 reflectivity spectrum shows a light blue-shift, probably due to a mismatch of deeper layer thickness.

#69949 - $15.00 USD Received 14 April 2006; revised 13 June 2006; accepted 14 June 2006

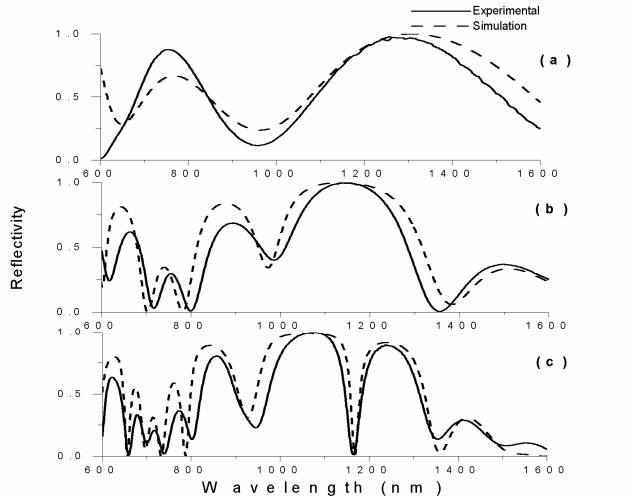

Fig.4. Experimental (solid curves) and calculate (dashed curves) reflectivity for S_3 T-M structure (a), S_4 T-M structure (b) and S_5 T-M structure (c). The measurements have been taken at normal incidence.

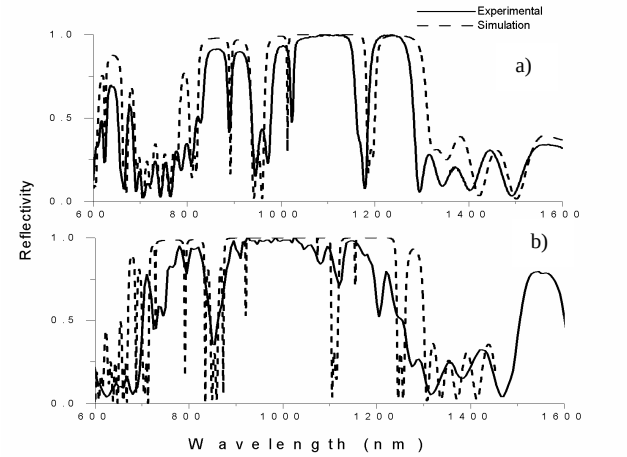

Fig. 5. Experimental (solid curves) and calculate (dash curves) reflectivity for S_6 T-M structure (a) and S_7 T-M structure (b). The measurements have been taken at normal incidence.

We have investigated the experimental reflectivity spectra of the S_6 and S_7 for both the TE (solid curve) and the TM (dashed curve) polarization at different incident angles up to 45° since they show the larger PBG, θ_2, of all. The results are reported in Figs. 6 and 7.The grey area highlights a PBG region of 70 nm, centered at 1100 nm which exists in the incident angle range between 0 and 30° in case of S_6. An even more extend PBG respect to the previous sequence, of about 90 nm, centered at 950 nm in the angular range between 0°-30° can be observed for S_7.

#69949 - $15.00 USD Received 14 April 2006; revised 13 June 2006; accepted 14 June 2006

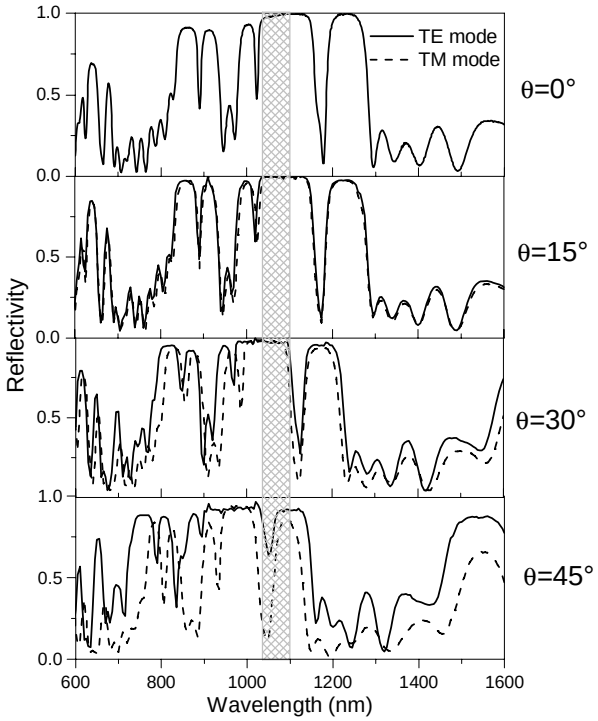

Fig. 6. Experimental reflectivity spectra of S_6 T-M structure for TE mode (solid curves) and TM mode (dashed curves) for different incident angles.

#69949 - $15.00 USD Received 14 April 2006; revised 13 June 2006; accepted 14 June 2006

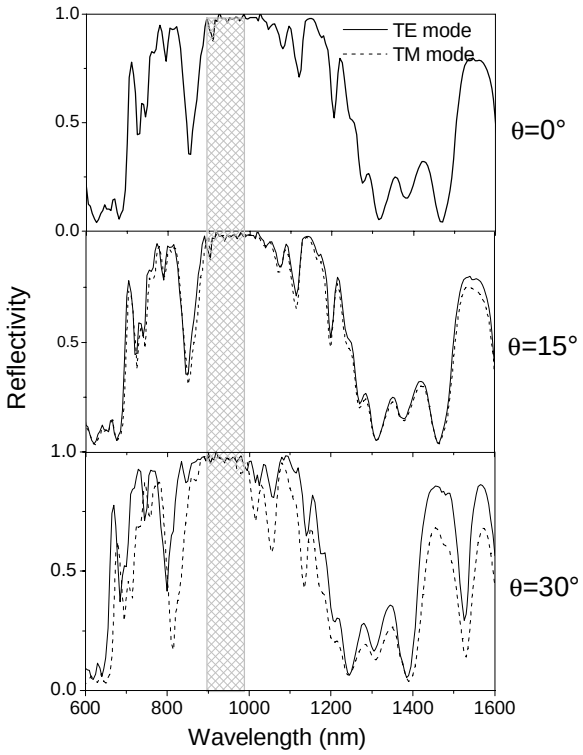

Fig. 7. Experimental reflectivity spectra of S_7 for TE mode (solid curve) and TM mode (dashed curve) for different incident angles.

5. Conclusions

In this work we have reported a theoretical approach to photonic bandgap analysis of 1D T-M structures. Furthermore the fabrication and the optical characterization of aperiodic Thue-Morse structures up to 128 layers based on the PSi technology have been reported. The multilayers exploit a high quality optical response and a good agreement between theoretical and experimental results has been obtained. We have found the splitting of the PBG on increasing of the T-M order. Partial PBG regions wide 70 nm and 90 nm, included between 0° and 30°, are observed for the S_6 and S_7 T-M structures, respectively. Even if it is not possible to obtain an omidirectional PBG with a T-M structures as in the case of Bragg mirrors [5], due to the low contrast between the high and low refractive index of the layers available, on the other hand, this kind of QC can be customized to show PBGs over a very large interval of wavelengths by properly modifying the refractive index and the thickness of the PSi layers.

#69949 - $15.00 USD Received 14 April 2006; revised 13 June 2006; accepted 14 June 2006